Bull Mater Sci (2020) 43:235
https://doi.org/10.1007/s12034-020-02204-5

Application of $k \cdot p$ method on band structure of GaAs obtained through joint density-functional theory

WAQAS MAHMOOD* and **BING DONG**
School of Physics and Astronomy, Shanghai Jiao Tong University, Shanghai 200240, People's Republic of China
*Author for correspondence (waqasmahmoodqau@sjtu.edu.cn)

MS received 23 November 2019; accepted 16 January 2020

Abstract. The structural and electronic properties of zinc-blende GaAs were calculated within the framework of plane-wave density-functional theory code JDFTx by using Becke 86 in 2D and PBE exchange-correlation functionals from libXC. The standard optimized norm-conserving Vanderbilt pseudopotentials were used to calculate optimized lattice constants, band gap and spin–orbit (SO) split-off parameter. The calculated values of optimized lattice constants and direct band gap are in satisfactory agreement with other published theoretical and experimental findings. By including SO coupling, conduction bands and valence bands were studied under parabolicity to calculate effective masses. The calculated values of effective masses and SO split-off parameter are in satisfactory agreement with most recent findings. This study will be useful for more computational studies related to semiconductor spintronic devices.

Keywords. JDFTx; zinc-blende GaAs; spin–orbit coupling; density-functional theory (DFT); norm-conserving pseudopotentials.

1. Introduction

The electron-spin interactions give rise to interesting semiconductor spintronic effects and allow us to control charge and spin [1,2]. In group III–V semiconductors, spin–orbit (SO) coupling manifests itself in band structure by splitting energy bands and preserving spin degeneracy as space inversion symmetry is not present in the primitive cell of these semiconductors [3]. A lack of space inversion symmetry generates momentum dependent SO field in analogy to the Zeeman field that splits energy bands. In zinc-blende (ZB) semiconductors, splitting can be described by cubic Dresselhaus field away from the zone centre [4]. The value of Dresselhaus coupling for GaAs lies between 9 and 28 eV $Å^3$. Experimentally, it is difficult to determine these parameters, however, theoretically accurate calculation of electronic band structure is required [2]. The incorporation of SO coupling improves the description of band structure and gives rise to many interesting phenomena in semiconductors such as spin relaxation [5], spin orientation (optical) [6], spin Hall effect [7], spin galvanic phenomena [8], etc.

The electronic properties of these semiconductors have been studied experimentally [9–13] and theoretically [14–21] by several authors; however, in all calculations within the formulism of density-functional theory (DFT), band gap is underestimated. The strongly underestimated fundamental band gap in GaAs [22] yields spin-splitting parameter (Δ_{SO}) 14 times larger in comparison with the value predicted by GW band structure [23]. To obtain a band gap that is consistent with experiment, it is necessary to acquire complete information about band structure including SO coupling [23–25].

This can be achieved through JDFTx which is an open-source plane-wave DFT software with rich features for DFT calculations. The designed strategy of the software allows us to write easy-to-read codes specially for DFT calculations and libjdftx helps in linking it with other codes. The code has been successfully used in electronic structure method development for exact exchange [26], X-ray measurements [27] and electron–phonon interactions [28]. Sundararaman *et al* [29] employed JDFTx with full-relativistic norm-conserving pseudopotentials and theoretically predicted hot carrier generation from surface plasmon decay. In another study, the authors used JDFTx to perform first-principles calculations on electrostatic potentials for reliable alignment at interfaces and defects [30]. Sun compared lattice constants, pristine surface energies and relative stability of pyrite and marcasite between VASP and JDFTx [31]. The results using JDFTx are in excellent agreement with the findings of VASP.

Furthermore, SO split-off parameter should be carefully calculated and this can be achieved by using phenomenological approach of $\boldsymbol{k} \cdot \boldsymbol{p}$ method [32,33]. In the $\boldsymbol{k} \cdot \boldsymbol{p}$ method, Hamiltonian is constructed by employing

Published online: 20 August 2020

perturbation theory [34,35] and group theory analysis is used to reduce the number of matrix elements which are replaced by effective parameters. The number of these parameters rely on the number of selected bands and on the symmetry of the described crystal. In ZB crystals, effective masses themselves allow the calculation of effective mass parameters [36]. Theoretically, effective masses can be determined by fitting parabolic dispersion near Γ point in the band structure [37,38].

In this paper, we study structural and electronic properties of ZB cubic phase GaAs in plane-wave DFT code JDFTx, by employing Becke 86 in 2D and PBE exchange-correlation functionals from libXC. We included SO coupling by using full relativistic norm-conserving pseudopotentials and further applied the $\boldsymbol{k} \cdot \boldsymbol{p}$ method to fit conduction (CBs) and valence bands (VBs) to calculate the effective masses of non-degenerate and degenerate bands. Our results compare fairly well with the existing findings and provide useful data for more empirical approaches.

The paper is organized as follows. Crystal structure of GaAs is shown in section 2. Computational method is given in section 3. Results are presented in section 4 with discussion and comparison. The last section concludes our study.

2. Crystal structure

GaAs is a binary alloy of the III–V semiconductor group. The atoms arranged in the ZB structure have tetrahedral coordination with two interpenetrating face-centred Bravais lattices, each with different atomic species. One species is cation whereas the other is anion. The particular order of cations and anions within unit cell determines spin orientation [24] caused by the SO field. The crystal structure of F-43M ZB GaAs is shown in figure 1 with Ga (cation) atoms positioned at origin and As (anion) atoms located at fractional coordinates (1/4, 1/4, 1/4) in a cubic lattice of length a.

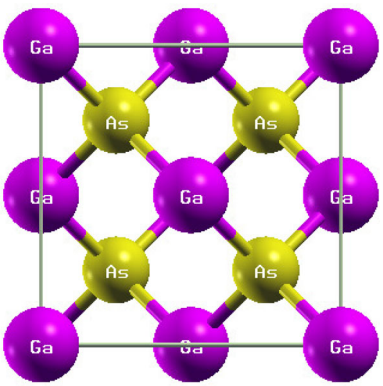

Figure 1. Crystal structure of F-43M ZB 3D-cubic GaAs.

3. Computational method

The exchange-correlation energy of electrons was represented by Becke 86 in 2D [39] and Perdew *et al* [40] from libXC [41] in JDFTx [42]. The valence electron–ion interactions were represented by optimized norm-conserving Vanderbilt pseudopotentials (ONCVPSP) [43] in the UPF format [44]. We performed calculations with no-spin and relativistic spin-type to calculate the structural and electronic properties of GaAs. The strain tensor was minimized to determine optimized lattice constants, and after complete convergence study, energy cutoff of 50 Ha and k-points grid [45,46] of $20 \times 20 \times 20$ that was less than 0.0001 mHa converged were selected. The optimized lattice constant was used to calculate band structure with and without SO coupling.

4. Results and discussion

4.1 *Structural properties*

The optimized lattice constant calculated by employing the L-BFGS scheme [47] was 5.711 Å that is 1% off from the experimentally determined value of 5.654 Å which is quite reasonable when the PBE exchange-correlation functional is used. Although the optimized lattice constant is 1% off from experiment, however, it is in satisfactory agreement with earlier reported findings. The comparison of our calculated value with earlier published theoretical and experimental values is given in table 1.

4.2 *Band structure*

4.2a *No spin–orbit*: Most of the DFT software underestimate lattice constants, however, this was not the case with JDFTx; therefore, we used it to calculate the band structure. The band dispersion of GaAs was calculated without SO coupling along the high symmetry path W–L–G–X–W–K and X–G–K using a primitive cell of two atoms. The symmetry point G represents zone centre Γ. The direct band gap ($E[\Gamma_{6c}] - E[\Gamma_{8v}]$) between CB Γ_{6c} and VB Γ_{8v} at zone centre Γ was 1.5480 eV. The gap of L-valley was 2.4569 eV and the gap of X-valley was 3.3398 eV. The gap ($E[\Gamma_{8c}] - E[\Gamma_{8v}]$) between CB Γ_{8c} and VB Γ_{8v} was

Table 1. Comparison of our calculated lattice parameter with reported findings.

Parameter	This work	Theoretical	Exp.
a	5.711	5.508[a], 5.651[b] 5.726[c], 5.755[d]	5.654[e] 5.653[f]

The lattice constant is in units of Å. [a]Ref. [48]; [b]ref. [49]; [c]ref. [50]; [d]ref. [51]; [e]ref. [52]; [f]ref. [53].

4.8660 eV. The gap ($E[\Gamma_{6c}] - E[\Gamma_{6v}]$) between CB Γ_{6c} and VB Γ_{6v} was 13.5645 eV. The gap ($E[\Gamma_{6v}] - E[\Gamma_{8v}]$) between VB Γ_{6v} and VB Γ_{8v} was −12.0165 eV. The band dispersion without SO coupling along the symmetry points W–L–G–X–W–K and X–G–K is shown in figure 2a and b, respectively. The calculated band gap is in fair agreement with recently reported finding [54].

4.2b *Spin–orbit*: The SO coupling was included by incorporating full relativistic optimized norm-conserving Vanderbilt pseudopotentials. The band structure was calculated along the high symmetry path W–L–G–X–W–K and X–G–K. The direct band gap ($E[\Gamma_{6c}] - E[\Gamma_{8v}]$) between CB Γ_{6c} and VB Γ_{8v} at zone centre Γ was 1.5142 eV. The gap of L-valley was 2.3873 eV and the gap of X-valley was 3.2496 eV. The gap ($E[\Gamma_{8c}] - E[\Gamma_{8v}]$) between CB Γ_{8c} and VB Γ_{8v} was 4.8272 eV. The gap ($E[\Gamma_{6c}] - E[\Gamma_{6v}]$) between CB Γ_{6c} and VB Γ_{6v} was 13.5529 eV. The gap ($E[\Gamma_{6v}] - E[\Gamma_{8v}]$) between VB Γ_{6v} and VB Γ_{8v} was −12.0387 eV. The SO split-off parameter was 0.3440 eV. The bands dispersion with SO coupling along the high symmetry points W–L–G–X–W–K and X–G–K is shown in figure 3a and b, respectively. The direct manifestation of SO coupling in band structure is splitting of valence energy bands into light-hole (LH), heavy-hole (HH) and SO split-off hole bands. Furthermore, the calculated values using JDFTx are not overestimated but in good agreement with the recently reported finding [54].

4.3 *Effective mass from* $\boldsymbol{k} \cdot \boldsymbol{p}$ *parameters*

The effective mass of the non-degenerate band can be calculated by using the $\boldsymbol{k} \cdot \boldsymbol{p}$ method. The complete information of the method is given in ref. [55]. By employing standard non-degenerate perturbation theory, eigenfunctions u_{nk} and eigenvalues E_{nk} at a neighbouring point $\boldsymbol{k}$ are expanded up to second order in $\boldsymbol{k}$ in terms of unperturbed wave functions u_{n0} and energies E_{n0}. Let us consider the lowest CB at the zone centre that has symmetry Γ_1.

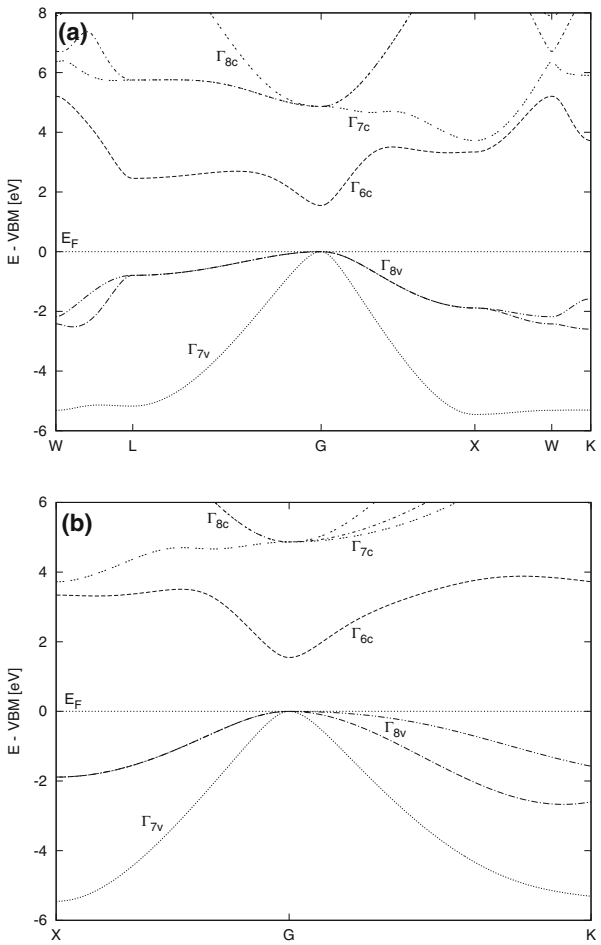

Figure 2. Bands dispersion of GaAs without SO coupling: (**a**) along path W–L–G–X–W–K and (**b**) along path X–G–K. The Fermi level is shown as E_F.

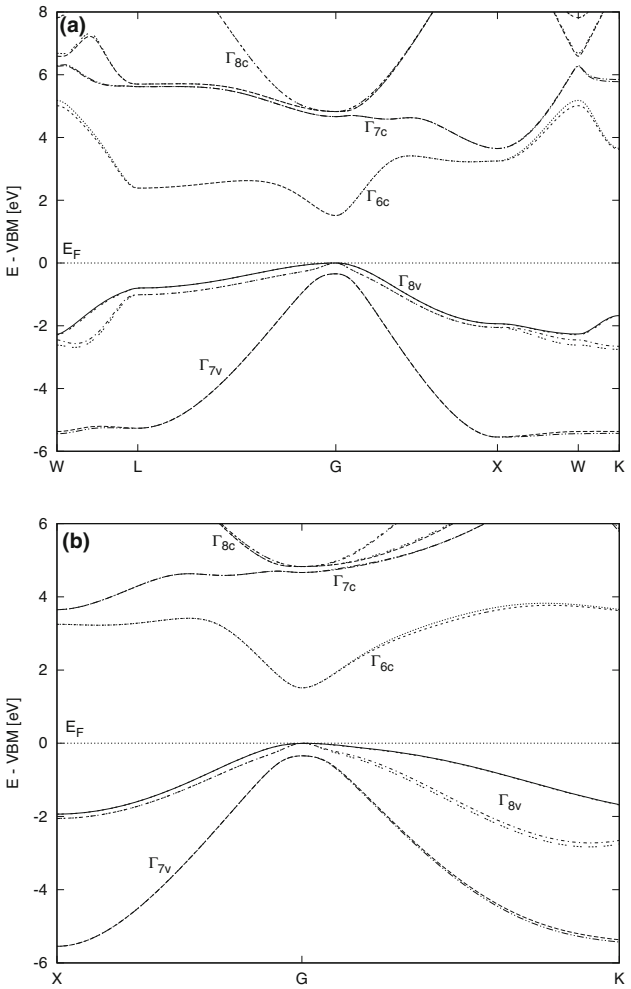

Figure 3. Bands dispersion of GaAs with SO coupling: (**a**) along path W–L–G–X–W–K and (**b**) along path X–G–K. The Fermi level is shown as E_F.

According to the $\boldsymbol{k}\cdot\boldsymbol{p}$ method, the effective mass can be determined mainly through its coupling to the nearest bands with Γ_4 symmetry, *via* the $\boldsymbol{k}\cdot\boldsymbol{p}$ term. These bands include both CBs and VBs. The momentum matrix element between Γ_1 CB and Γ_4 CB is smaller in comparison with the momentum matrix element between Γ_1 CB and Γ_4 VB. Therefore, for III–V group semiconductors, under the conditions of parabolicity at the extreme band edge of the CB, we have

$$\frac{m}{m_c^*} \approx \frac{2P^2}{mE_0}, \tag{1}$$

where E_0 is the direct separation between the CB and VB, i.e., the band gap of the material and the matrix element P^2 is approximately the same for III–V semiconductors with $2P^2/m \approx 20$ eV [55]. The CB band minimum at the zone centre satisfies the condition of parabolicity and its minimum is the minimum of parabola fit within 5% of first Brillouin zone. Therefore, the CB effective mass (m_c^*) was calculated by using equation (1). The calculated effective mass of CB (m_c^*) was $0.0525m$, that is in fair agreement with the reported value in ref. [55].

To calculate the effective mass of the degenerate band at the VB extremum at the zone centre, we used 6×6 ZB effective $\boldsymbol{k}\cdot\boldsymbol{p}$ Hamiltonians proposed by Luttinger and Kohn (LK6) [56] and extended by Kane [32] to an 8×8 model. According to the LK6 model, class A is composed of three top most VBs such as HH, LH and SO split-off hole near Γ point. Kane included the first CB in class A by using the same model and perturbative order. The Kane Hamiltonian depends on five different effective mass parameters such as $\tilde{\gamma}_1$, $\tilde{\gamma}_2$, $\tilde{\gamma}_3$, $\tilde{e}$ and P along with the band gap and Δ_{SO}. However, in the LK6 model, three parameters such as γ_1, γ_2 and γ_3 along with Δ_{SO} are important [34,35]. The authors in refs. [57,58] also used the $\boldsymbol{k}\cdot\boldsymbol{p}$ method and more recently Bastos *et al* [59] used electronic g-factors that are directly linked to the spin splitting of the carrier bands, to calculate the effective mass by using the values of E_P, E_{gap} and Δ_{SO} in Roth's formula [60] which is given by

$$g_c^* = 2 - \frac{2E_P\Delta_{SO}}{3E_{gap}(E_{gap}+\Delta_{SO})}, \tag{2}$$

Equation (2) only considers interaction between VB and CB. The interactions between other bands are neglected. The relationships between both model parameters are given by

$$\gamma_1 = \tilde{\gamma}_1 + \frac{E_p}{3E_{gap}}, \quad \gamma_2 = \tilde{\gamma}_2 + \frac{E_p}{6E_{gap}},$$
$$\gamma_3 = \tilde{\gamma}_3 + \frac{E_p}{6E_{gap}},$$
$$e = \tilde{e} + \frac{(E_{gap}+(2/3)\Delta_{SO})E_p}{E_{gap}(E_{gap}+\Delta_{SO})}, \quad E_p = \frac{2m_0}{\hbar^2}P^2. \tag{3}$$

Table 2. Comparison of our calculated values with Bastos *et al*'s results.

Parameter	This work	Ref. [59]
E_p	29.1250 eV	
γ_1	6.850	
γ_2	2.060	
γ_3	2.420	
$m_{lh[100]}$	0.0912	0.088
$m_{lh[110]}$	0.0855	0.079
$m_{hh[100]}$	0.3663	0.357
$m_{hh[110]}$	0.4975	0.672
$m_{lh[111]}$	0.0868	0.076
$m_{hh[111]}$	0.4588	0.898
m_{SO}	0.1766	0.169
g_c^*	− 0.37	− 0.34
Δ_{SO}	0.3440	0.325–0.365

The effective masses as determined from these parameters are given by the relations

$$m_{lh}[100] = (\gamma_1+2\gamma_2)^{-1}, \quad m_{lh}[110] = (\gamma_1+2\gamma_3)^{-1},$$
$$m_{hh}[100] = (\gamma_1-2\gamma_2)^{-1}, \quad m_{hh}[110] = (\gamma_1-2\gamma_3)^{-1},$$
$$m_{lh}[111] = (\gamma_1+\sqrt{(\gamma_2^2+3\gamma_3^2)})^{-1}, \quad m_e = e^{-1},$$
$$m_{hh}[111] = (\gamma_1-\sqrt{(\gamma_2^2+3\gamma_3^2)})^{-1},$$
$$m_{SO} = \left(\gamma_1 - \frac{1}{3}\frac{\Delta_{SO}E_p}{E_{gap}(E_{gap}+\Delta_{SO})}\right)^{-1}. \tag{4}$$

The effective masses of degenerate VBs along the [100], [110] and [111] directions were calculated by using the aforementioned relationships and the results are tabulated in table 2. For the comparison, the results of Bastos *et al* [59] are given. Our calculated value of Δ_{SO} was 0.34 eV that is in satisfactory agreement with the value reported in ref. [59,61].

5. Conclusion

We studied the structural and electronic properties of ZB cubic phase GaAs by employing Becke 86 in 2D and PBE exchange-correlation functionals. Several authors have reported theoretical results on GaAs by using GGA and ultrasoft pseudopotentials with underestimated band gap and overestimated spin-splitting parameters; however, we used standard ONCVPSP in plane-wave joint DFT code. The optimized lattice constant of 5.711 Å obtained using the L-BFGS algorithm is 1% off from the experimental value of 5.654 Å [52] and it is in fair agreement with the theoretical value of 5.742 Å [59]. The band gap of 1.5142 eV with SO coupling and SO split-off parameter in excellent agreement with experiment [59,61]. The effective mass parameters

calculated using the $\boldsymbol{k} \cdot \boldsymbol{p}$ method are in fair agreement with most recent findings of Bastos *et al* [59]. Our findings provide useful data for further empirical studies related to semiconductor spintronic devices. Finally, we have used open source code JDFTx in our calculations that has recently been introduced and we predict that its accuracy is quite reasonable.

Acknowledgement

This work was supported by the National Science Foundation of China under Grant No. 11674223.

References

[1] Žutić I, Fabian J and Sarma S D 2004 *Rev. Mod. Phys.* **76** 323
[2] Fabian J, Matos-Abiague A, Ertler C, Stano P and Žutić I 2007 *Acta Phys. Slovaca* **57** 565
[3] Campos T, Junior P E F, Gmitra M, Sipahi G M and Fabian J 2018 *Phys. Rev. B* **97** 245402
[4] Dresselhaus G 1955 *Phys. Rev.* **100** 580
[5] Fabian J and Sarma S D 1999 *J. Vac. Sci. Technol. B* **17** 1708
[6] Meier F and Zakharchenya B P 2012 *Optical orientation* (North-Holland: Elsevier)
[7] Sinova J, Valenzuela S O, Wunderlich J, Back C H and Jungwirth T 2015 *Rev. Mod. Phys.* **87** 1213
[8] Ganichev S D 2008 *Int. J. Mod. Phys. B* **22** 1
[9] Fern R E and Onton A 1971 *J. Appl. Phys.* **42** 3499
[10] Adachi S 1987 *Phys. Rev. B* **35** 7454
[11] Joyce H J, Docherty C J, Gao Q, Tan H H, Jagadish C, Lloyd-Hughes J *et al* 2013 *Nanotechnology* **24** 214006
[12] Garriga M, Lautenschlager P, Cardona M and Ploog K 1987 *Solid State Commun.* **61** 157
[13] Djurišić A B, Rakić A D, Kwok P C, Li E H and Majewski M L 1999 *J. Appl. Phys.* **85** 3638
[14] Remediakis I N and Kaxiras E 1999 *Phys. Rev. B* **59** 5536
[15] Lebègue S, Arnaud B, Alouani M and Bloechl P E 2003 *Phys. Rev. B* **67** 155208
[16] Koller D, Tran F and Blaha P 2011 *Phys. Rev. B* **83** 195134
[17] Tomić S, Montanari B and Harrison N M 2008 *Physica E* **40** 2125
[18] Shimazaki T and Asai Y 2010 *J. Chem. Phys.* **132** 224105
[19] Kim Y S, Marsman M, Kresse G, Tran F and Blaha P 2010 *Phys. Rev. B* **82** 205212
[20] Wang Y, Yin H, Cao R, Zahid F, Zhu Y, Liu L *et al* 2013 *Phys. Rev. B* **87** 235203
[21] Hinuma Y, Grüneis A, Kresse G and Oba F 2014 *Phys. Rev. B* **90** 155405
[22] Perdew J P and Zunger A 1981 *Phys. Rev. B* **23** 5048
[23] Chantis A N, van Schilfgaarde M and Kotani T 2006 *Phys. Rev. Lett.* **96** 086405
[24] Cardona M, Christensen N E and Fasol G 1988 *Phys. Rev. B* **38** 1806
[25] Winkler R 2003 *Spin–orbit coupling effects in two-dimensional electron and hole systems* (Berlin: Springer)
[26] Sundararaman R and Arias T A 2013 *Phys. Rev. B* **87** 165122
[27] Plaza M, Huang X, Ko J Y P, Shen M, Simpson B H, Rodríguez-Löpez J *et al* 2016 *J. Am. Chem. Soc.* **138** 7816
[28] Brown A M, Sundararaman R, Narang P, Goddard III W A and Atwater H A 2016 *ACS Nano* **10** 957
[29] Sundararaman R, Narang P, Jermyn A S, Goddard III W A and Atwater H A 2014 *Nat. Commun.* **5** 5788
[30] Sundararaman R and Ping Y 2017 *J. Chem. Phys.* **146** 104109
[31] Sun R 2013 *Doctoral dissertation* (Massachusetts Institute of Technology)
[32] Kane E 1966 in *Semiconductors and semimetals* R Willardson and A C Beer (eds) vol 1 (Amsterdam: Elsevier) p 75
[33] Sipahi G M, Enderlein R, Scolfaro L M R, Leite J R, da Silva E C F and Levine A 1998 *Phys. Rev. B* **57** 9168
[34] Enderlein R and Horing N J 1997 *Fundamentals of semiconductor physics and devices* (Singapore: World Scientific)
[35] Willatzen M and Voon L C L Y 2009 *The k ·p method* (Berlin: Springer)
[36] Enderlein R, Sipahi G M, Scolfaro L M and Leite J R 1998 *Phys. Status Solidi B* **206** 623
[37] Dugdale D J, Brand S and Abram R A 2000 *Phys. Rev. B* **61** 12933
[38] Ramos L E, Teles L K, Scolfaro L M R, Castineira J L P, Rosa A L and Leite J R 2001 *Phys. Rev. B* **63** 165210
[39] Vilhena J G and Marques M A L 2014 unpublished
[40] Perdew J P, Burke K and Ernzerhof M 1996 *Phys. Rev. Lett.* **77** 3865
[41] Marques M A L, Oliveira M J T and Burnus T 2012 *Comput. Phys. Commun.* **183** 2272
[42] Sundararaman R, Letchworth-Weaver K, Schwarz K A, Gunceler D, Ozhabes Y and Arias T A 2017 *SoftwareX* **6** 278
[43] Hamann D R 2013 *Phys. Rev. B* **88** 085117
[44] van Setten M J, Giantomassi M, Bousquet E, Verstraete M J, Hamann D R, Gonze X *et al* 2018 *Comput. Phys. Commun.* **226** 39
[45] Monkhorst H J and Pack J D 1976 *Phys. Rev. B* **13** 5188
[46] Pack J D and Monkhorst H J 1977 *Phys. Rev. B* **16** 1748
[47] Liu D C and Nocedal J 1989 *Math. Programm.* **45** 503
[48] Agrawal B K, Yadav P S, Kumar S and Agrawal S 1995-I *Phys. Rev. B* **52** 4896
[49] Min B I, Massidda S and Freeman A J 1988 *Phys. Rev. B* **38** 1970
[50] Staroverov V N, Scuseria G E, Tao J and Perdew J P 2004 *Phys. Rev. B* **69** 075102
[51] Kalvoda S, Paulus B, Fulde P and Stoll H 1997 *Phys. Rev. B* **55** 4027
[52] Vurgaftman I, Meyer J R and Ram-Mohan L R 2001 *J. Appl. Phys.* **89** 5815
[53] Filippi C, Singh D J and Umrigar C J 1994 *Phys. Rev. B* **50** 14947
[54] Ali M A, Khan N, Ahmad F, Ali A and Ayaz M 2019 *Bull. Mater. Sci.* **42** 36
[55] Yu P Y and Cardona M 2010 *Fundamentals of semiconductors: physics and materials properties* (New York: Springer)
[56] Luttinger J M and Kohn W 1955 *Phys. Rev.* **97** 869
[57] Gmitra M and Fabian J 2016 *Phys. Rev. B* **94** 165202
[58] Bastos C M, Sabino F P, Junior P E, Campos T, Da Silva J L and Sipahi G M 2016 *Semicond. Sci. Technol.* **31** 105002
[59] Bastos C M, Sabino F P, Sipahi G M and Da Silva J L 2018 *J. Appl. Phys.* **123** 065702
[60] Roth L M, Lax B and Zwerdling S 1959 *Phys. Rev.* **114** 90
[61] Madelung O 2004 *Semiconductors: data handbook* (Berlin: Springer)